THE JOURNAL OF PHYSICAL CHEMISTRY B

Article

pubs.acs.org/JPCB

Formation of Two Different Types of Oligomers in the Early Phase of pH-Induced Aggregation of the Alzheimer Aβ(12-28) Peptide

Paulami Mandal, Nadejda Eremina, and Andreas Barth*

Stockholm University, Department of Biochemistry and Biophysics, Arrhenius Laboratories, 10691 Stockholm, Sweden

Supporting Information

ABSTRACT: The early phase in the aggregation process of the Alzheimer's peptide Aβ(12-28) with both protected and unprotected ends was studied by time-resolved infrared spectroscopy and circular dichroism spectroscopy. Aggregation in the time-resolved experiments was initiated by a rapid pH drop caused by the photolysis of 1-(2-nitrophenyl)ethyl sulfate (caged sulfate). The infrared spectra indicate two different types of aggregates from both versions of the Aβ(12-28) peptide. One type has small and/or twisted β sheets with a β-sheet band at 1627 cm^{-1}. They form fast (within 60 ms), presumably from initial aggregates, and their spectral signature is consistent with a β-barrel structure. The other type arises relatively slowly from unstructured monomers on the seconds-to-minutes time scale and forms at lower pH than the first type. These β sheets are antiparallel, planar, and large and show an absorption band at 1622 cm^{-1} that shifts to 1617 cm^{-1} in 12 min with most of the shift occurring in 10 s.

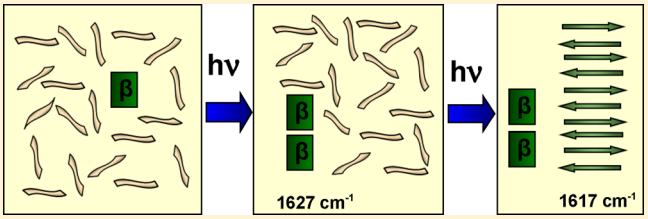

INTRODUCTION

Alzheimer's disease (AD) is the most frequent, widespread neurodegenerative disorder with the distinct characteristic of the progressive deposition of extracellular fibrillar amyloids in the brain.[1] In AD, the major component of the amyloid fibrils is named amyloid β (Aβ) or Alzheimer's peptide and is formed by the enzymatic cleavage from the β-amyloid precursor protein (APP). The Aβ peptide is 39−43 residues long and has a tendency to aggregate to insoluble amyloid fibrils from an aqueous solution, which depends on various parameters, such as peptide concentration, temperature, ionic conditions of the solvent, and pH.[2−4] This involves a transformation of the secondary structure from mostly a random coil to a β-sheet structure.[5−7] In general, Aβ(1-42) and Aβ(1-40) form fibrils with parallel β sheets, but shorter fragments have a propensity to form antiparallel β sheets.[8−14] Recent evidence has indicated that soluble Aβ oligomers and protofibrils, which occur at an intermediate stage of the fibril formation, may be the actual source of neurotoxicity in AD-like diseases instead of the insoluble fibrils.[15−18] Because of their neurotoxic nature and their role as nucleus or template in the aggregation process, oligomers have recently gained considerable attention, and it has become important now to characterize not only the oligomeric structures but also the structural changes accompanying their assembly at the molecular level in order to better understand the cause of AD. In studies, where the Aβ oligomers were in a nonaqueous environment, they consist of antiparallel β sheets, whereas the fibrils are composed of parallel β sheets.[19,20]

Circular dichroism (CD) and Fourier transform infrared spectroscopy (FTIR) are two powerful methods for the determination of the secondary structure changes during Aβ oligomerization and fibrillization. CD spectroscopy is most useful in distinguishing a random coil from an α helix and β sheets.[21−24] FTIR spectroscopy is a complementary method to CD that is able to discriminate clearly between a β-sheet structure and a random coil or α-helix structure. It can, in certain cases, distinguish between parallel and antiparallel β sheets, although the discrimination is less clear-cut than previously thought and the position of the main band in the 1640−1610 cm^{-1} range cannot be used for this purpose.[25,26] A high wavenumber component (∼1690 cm^{-1}) of the amide I absorption appears for planar antiparallel β sheets with a large number of strands, but not for small or twisted antiparallel sheets. The band is weak or not observable for proteins with parallel β sheets,[27,28] with the exception of β-helix proteins.[27] Accordingly, it is not present in spectra of Aβ(1-42) aggregates and fibrils obtained by us[40] and others.[19] Simulations of the amide I absorption of parallel β sheets indicate a tail of absorption that can smear out up to ∼50 cm^{-1} from the main band to high wavenumbers.[29−32] There is some discrepancy between different simulations regarding the splitting between the main band at low wavenumber and the strongest sideband at higher wavenumber. While Hahn et al.[29] find a similar splitting for comparable parallel and antiparallel sheets, others find smaller splittings for parallel sheets.[31,32] However, a distinct band at high wavenumber (∼1690 cm^{-1}), clearly separated from the remaining amide I absorption, has neither been observed experimentally nor predicted theoretically for parallel sheets. Therefore, a high wavenumber component with

Received: May 23, 2012
Revised: September 14, 2012
Published: September 14, 2012

this property serves as a marker band for antiparallel β sheets that are large and planar, and this has been exploited previously for structural assignment.[19,33,34] FTIR spectroscopy has been used extensively to study aggregation processes, secondary structure transitions, and folding of peptides and proteins, especially in the field of amyloid proteins.[19,35−39] For the Aβ peptide, it has determined secondary structures and slow structural conversion kinetics for both full length peptides and shorter fragments.

To increase the time resolution of infrared spectroscopic studies of peptide aggregation, we triggered aggregation in previous work[40] by a pH jump caused by photolysis of 1-(2-nitrophenyl)ethyl sulfate (NPE sulfate), a biologically inactive compound that releases a proton on the microsecond time scale upon UV irradiation, resulting in a potentially large pH jump (Scheme 1).[41] NPE sulfate is an example for so-called caged compounds, which have been used in FTIR spectroscopy to study biological reactions for 20 years.[42−45] The pH drop technique has the advantage that the formation of oligomers can be followed in an aqueous solution in contrast to conventional absorption spectroscopy.

Scheme 1. Photolysis Reaction of 1-(2-Nitrophenyl)ethyl Sulfate (NPE Sulfate)

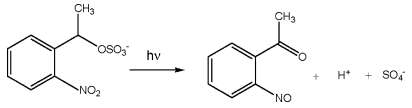

In our present study, we investigated the formation of early oligomers of the Aβ(12-28) peptide, which consists of residues important for the transition into the β-sheet-enriched conformation and for amyloid formation.[46,47] The peptide forms amyloid-like fibrils,[46,48] promoted by slightly acidic pH,[46] and its aggregates are cytotoxic.[49] Its small size makes it well amenable to molecular dynamics simulations,[50,51] and it, therefore, presents an important link between simulations and experiments. Here, FTIR spectroscopy was employed to follow the early phase of Aβ aggregation induced by a sudden pH jump. We used two different variants with protected (Aβ(12-28)$_p$) and unprotected (Aβ(12-28)$_u$) ends. In the protected peptide, there is little electrostatic effect from its two uncharged ends, like in the respective section contained in the full-length peptide. However, the ends are charged in the unprotected version, which might affect aggregation and even dictate the relative orientation of neighboring strands in the β sheet. Nevertheless, protected and unprotected peptides have been used in biophysical studies, assuming that the unprotected peptides are representative for the respective portion in the full-length peptide despite the charges at the ends. Our aims were to study the effect of charged and uncharged ends of the peptide in the aggregation process and to observe the time evolution of the association of β strands in each case.

We observed formation of at least two different types of antiparallel β sheets in the early stage of aggregation for both Aβ(12-28)$_p$ and Aβ(12-28)$_u$, which differ in their amide I maximum, pH profile, kinetics of formation, size, and ability to grow. One type corresponds to small and/or twisted β sheets, forming fast from pre-existing aggregates, and the other relates to multistrand, more planar β sheets developing relatively slowly from monomeric peptides.

RESULTS

pH-Dependent Aggregation from CD and IR Absorption Spectra. To observe the influence of pH on the peptide, we measured CD as well as IR absorption spectra of the protected peptide at different pH values (2, 4, 6, 9) using the same sample in the same cuvette for both methods. Figure 1A shows the CD spectra of the peptide (400 μM). It appears from the CD spectra that there is a negative band around 196 nm for both pH 2 and pH 9, indicating the predominant presence of random coil structures at these pH values. In contrast, at pH 4, a negative band is evident at 217 nm with a positive band below 210 nm, indicating mostly β-sheet-rich conformations at this pH value. Also, for pH 6, the negative band at 216 nm suggests the presence of β sheets, although the random coil contribution seems to be more pronounced than at pH 4.

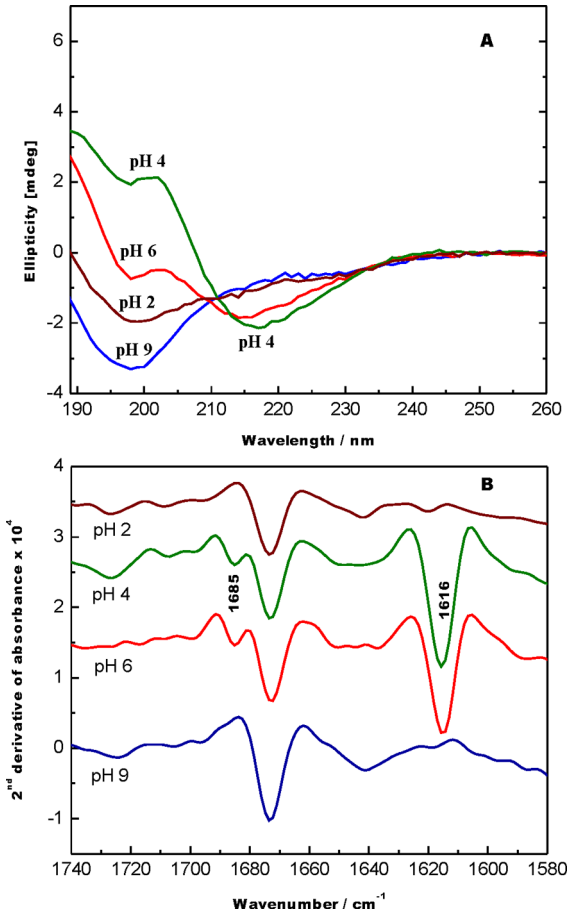

Figure 1. pH-dependent structural changes of Aβ(12-28)$_p$. (A) Circular dichroism spectra and (B) second derivative of IR absorbance spectra at pH 9.0 (blue), 6.0 (red), 4.0 (green), and 2.0 (brown). The spectra were shifted horizontally for a clearer presentation.

Figure 1B shows the second derivative of IR absorption spectra in the absorption region of the amide I vibration of the peptide backbone, which is sensitive to the secondary structure. Negative bands in second derivative spectra correspond to component bands in the absorption spectrum. In line with the CD results, a strong band present at 1616 cm^{-1} and a weak band at 1685 cm^{-1} at both pH 4 and pH 6 indicate the formation of antiparallel β sheets at these pH values, whereas no such bands were found at pH 2 and 9. A 24 h time series for the pH 6 sample revealed that these band positions did not

dx.doi.org/10.1021/jp305015g | J. Phys. Chem. B 2012, 116, 12389−12397

change over 24 h, indicating that the aggregates are stable over this time. The strong 1673 cm^{-1} band in all spectra can be assigned to the presence of trifluoroacetic acid (TFA) in the samples. Hence, both CD and IR absorption spectra suggest that the peptide, prepared separately for the various pH values from the same high pH stock solution, remains mostly in a random coil structure at pH 2 and 9 and transforms to a β-sheet-enriched structure at pH 4 and 6.

Time-Resolved FTIR Spectroscopy of Protected Aβ-(12-28). To promote the aggregation in the Aβ(12-28) peptide, a pH jump was induced by the flash photolysis of NPE sulfate, which releases a proton on the microsecond time scale. Figure 2A shows the difference spectra of $A\beta(12\text{-}28)_p$ aggregation upon the first photolysis flash. With the freshly prepared peptide (i.e., within 1 h), we found (Figure 2A) an intense broad positive band near 1627 cm^{-1} after the first flash, which we assign to β-sheet formation of the $A\beta(12\text{-}28)_p$ peptide from the known wavenumber dependence of the amide I absorption.[25,35,52] To reveal the time evolution of the $A\beta(12\text{-}28)_p$ bands, we evaluated the band area of several bands. The 1627 cm^{-1} band (Figure 2B) exhibits basically a step change with an initial phase that is faster than the time resolution of the measurements (60 ms). The control with NPE sulfate alone is also shown in the figure and demonstrates that NPE sulfate has an insignificant contribution at this band position. We observed also another positive band in Figure 2A at 1687 cm^{-1} and a weak band at 1601 cm^{-1}. These bands are at least partially due to the photolysis of NPE sulfate.[53] The band at 1687 cm^{-1} is assigned to the keto group and the weak band at 1601 cm^{-1} to a ring vibration of the photolysis byproduct 2-nitrosoacetophenon.[44,53,54]

Attempts to reveal a peptide contribution to the 1687 cm^{-1} band remained inconclusive. Subtracting either a photolysis spectrum of NPE sulfate at pH 8.2 in the absence of peptide or spectra with small peptide signals from spectra obtained with large peptide signals produced a very small band near 1697 cm^{-1} (not shown), which, because of its small amplitude, cannot be safely assigned to the peptide.

In the spectra recorded early after the photolysis flash, signals of the *aci*-nitro intermediate in the photolysis reaction were observed that decayed with a rate of 8 s^{-1}. Since the decay rate of this intermediate is pH-dependent, the signals could be used to determine the pH after the pH jump by comparing with the *aci*-nitro decay rate of buffered NPE sulfate samples (in 240 mM Mops). At pH 8.2, the measured decay rate was 10 s^{-1}, close to the rate determined in the unbuffered experiments with peptide. Therefore, we conclude that the pH is ~8.2 after the first flash in these peptide samples.

After the second flash, the pD was between 4 and 5, as indicated by pH paper. Interestingly, the second flash produced aggregates with different properties, as shown in Figure 2C: we obtained the β-sheet band initially at 1622 cm^{-1} (within 60 ms after the flash); it increased and shifted to 1617 cm^{-1} within 12 min (Figure 2C). Again, a band at 1687 cm^{-1} was observed, which was partly due to the photolysis reaction. When the photolysis contribution was subtracted using spectra with different ratios of peptide and photolysis signals (see Figure S1 in the Supporting Information), a band was still observed at this position in all phases of the reaction, initially at 1684 cm^{-1} and later shifting to 1686 cm^{-1}. The same result was obtained when a photolysis difference spectrum of NPE sulfate alone was subtracted (not shown). The presence of this band indicates the formation of antiparallel β sheets. It is interesting that its

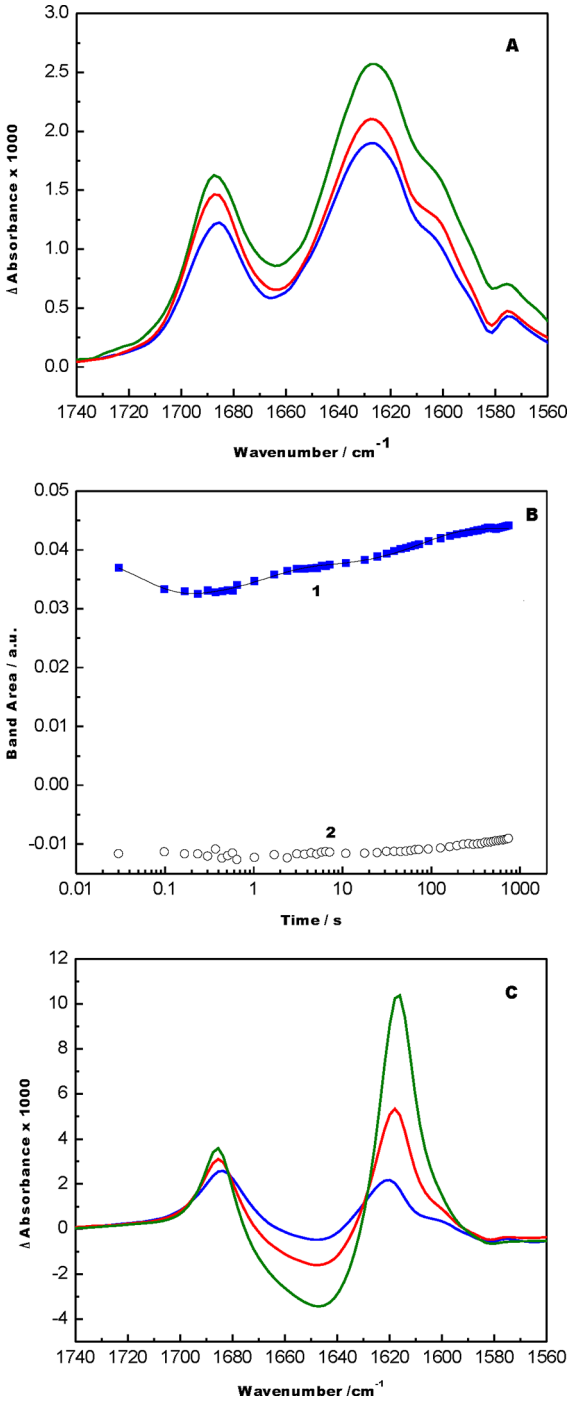

Figure 2. Infrared absorbance changes due to rapid acidification of $A\beta(12\text{-}28)_p$ samples by photolysis of NPE sulfate in D_2O. (A) Time-dependent spectral changes in the amide I band following the first photolysis flash. Spectra corresponding to the following time intervals: 0.002−0.674 s (blue), 0.69−7.5 s (red), 418−760 s (green). (B) Time evolution of the main β-sheet band at 1627 cm^{-1} in panel A (blue squares) and control with NPE sulfate alone (open circles). (C) Time-dependent spectral changes after the second photolysis flash. Recording times and color code are as those in panel A.

contribution relative to that of the main β-sheet band decreases with time.

It is also evident in Figure 2C that a large broad negative band from 1660 to 1630 cm^{-1} increases with time. This band is attributable to the disappearance of the random coil structure in

dx.doi.org/10.1021/jp305015g | J. Phys. Chem. B 2012, 116, 12389−12397

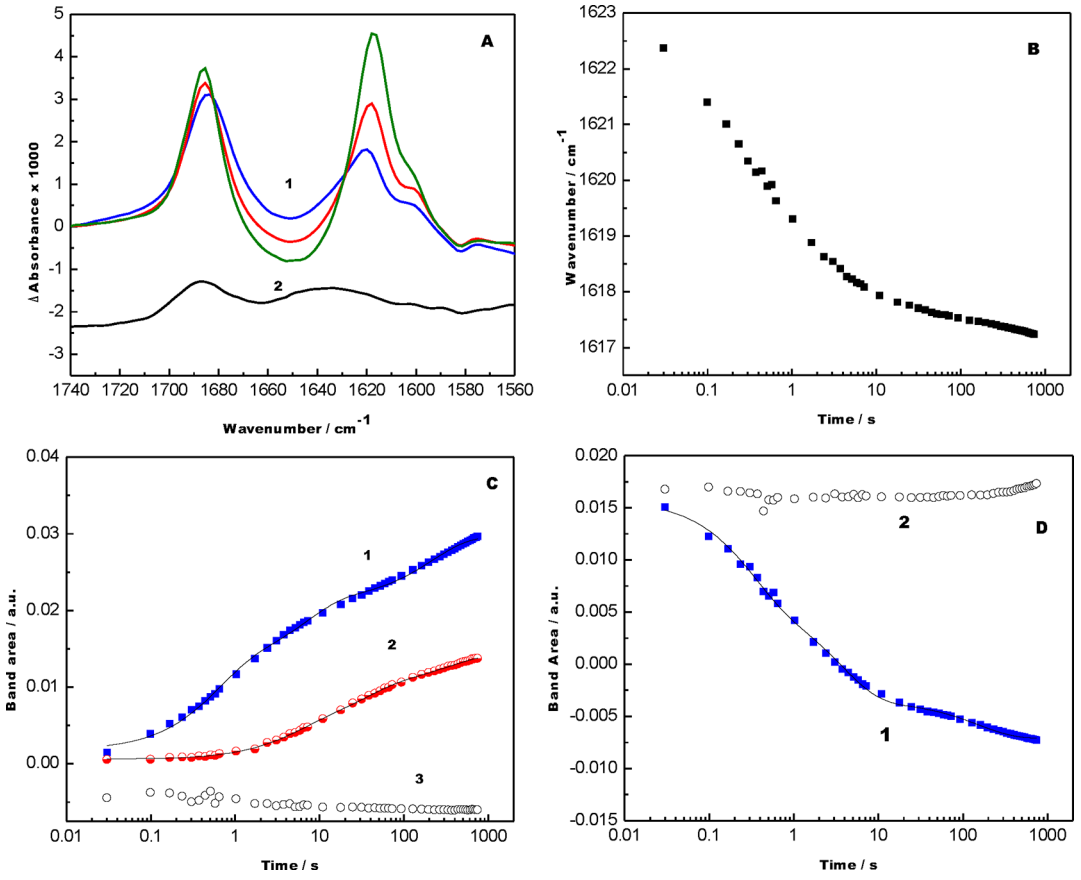

Figure 3. Effect of extra sonication on the aggregation process of Aβ(12-28)$_p$. (a) Time-dependent spectral changes in the amide I region after the first flash on a sample subjected to an additional 1 min of ice sonication. Spectra recording times and color code are as those in Figure 2A. The black spectrum is a control spectrum recorded 418−760 s after the photolysis flash in the presence of 100 mM TRIS buffer pH 9.5 in addition to peptide and NPE sulfate. The spectrum was shifted horizontally for a clearer presentation. (b) Spectral shift of the main β-sheet band as a function of time. (c) Time-evolution of the β-sheet band at 1617 cm^{-1} upon flash 1 (blue squares) and flash 2 (red circles) and triple-exponential fit. Open, black circles: control with NPE sulfate alone. (d) Time course of the loss of the random coil structure at 1645 cm^{-1} upon flash 1 (blue squares) and triple-exponential fit. Open circles: control with NPE sulfate alone.

the peptide, and its contribution relative to that of the main β-sheet band remains constant throughout the observation time. Noticeably, such a random coil band is absent in the first flash (Figure 2A).

The different spectral signatures obtained in flash 1 and flash 2 indicate that different β sheets with different aggregation kinetics are formed and we denote these as the *1627 cm^{-1} aggregates* and *1617 cm^{-1} aggregates*, respectively, according to the final band position of the β-sheet band. The 1627 cm^{-1} aggregates form much faster than the 1617 cm^{-1} aggregates (millisecond vs second time scale). Occasionally, the 1617 cm^{-1} aggregates were observed already after the first flash. This occurred in 20% of our experiments with fresh and stored samples, likely due to the difficulty of maintaining the pH in the unbuffered solutions required by our approach.

The peptide solution for the above experiments was prepared as described in the Materials and Methods. We have used the same peptide stock solution for our next set of experiments but applied an extra 1 min of ice sonication. Experiments with and without extra sonication were done on the same day. The spectra of the first pH drop with these extra-sonicated samples are shown in Figure 3A, and Figure 3B displays the time dependence of the position of the main β-sheet band. The spectra are similar to those obtained in the second pH drop for samples *without* extra sonication. Subtracting the photolysis signals as for the previous experiments also revealed in this case a high wavenumber component of peptide absorption at 1688 cm^{-1} (not shown). Similar features were observed upon the second flash, indicating formation of the same type of aggregates in both flashes with the extra-sonicated samples.

The 1617 cm^{-1}(Figure 3C) and 1643 cm^{-1} (Figure 3D) bands followed triple-exponential kinetics with time constants and relative amplitudes listed in Table 1. The control with NPE sulfate alone is also shown in the respective figures and demonstrates that NPE sulfate has insignificant contributions at these band positions. Noticeably, the 1617 cm^{-1} aggregates form considerably slower upon the second flash. This is probably due to less monomeric peptides being present.

Table 1. Fit Parameters for the Triple-Exponential Fits to the Time Course of Infrared Bands of Protected Aβ(12-28)[a]

flash no.	band position (cm^{-1})	A_1[b]	T_1[b] (s)	A_2[b]	T_2[b] (s)	A_3[b]	T_3[b] (s)
1	1617	0.39	0.58	0.31	6.6	0.30	217
	1643	0.45	0.32	0.40	3.9	0.15	158
2	1617	0.29	4.7	0.39	32	0.31	343

[a]Values are for the spectra of the extra-sonicated samples shown in Figure 3. [b]A_i = relative amplitudes; T_i = time constants.

dx.doi.org/10.1021/jp305015g | J. Phys. Chem. B 2012, 116, 12389−12397

Controls. Apart from recording spectra of the photolysis of NPE sulfate alone, we performed a further control experiment because the photolysis byproduct 2-nitrosoacetophenon is hydrophobic and might associate with the peptide and cause aggregation. To exclude that possibility, a control experiment was done in which 100 mM Tris buffer stabilized the pH at 9.5 with the extra-sonicated stock solution. After application of the flash, none of the peptide signals discussed above was observed in the 1660−1620 cm^{-1} region (black curve in Figure 3A), suggesting the absence of peptide aggregation. The remaining band at 1687 cm^{-1} is due to 2-nitrosoacetophenon. This observation demonstrates that it is only the pH jump that induces peptide aggregation and not the photolysis byproduct 2-nitrosoacetophenon.

Time-Resolved FTIR Spectroscopy of Unprotected Aβ(12-28). We also studied the aggregation of the unprotected variant $Aβ(12\text{-}28)_u$. Using 1 min of sonication, we got results similar to those with the extra-sonicated protected peptide: after both the first and the second flashes, we found the β-sheet band at ∼1620 cm^{-1} gradually increasing in amplitude and shifting toward lower wavenumbers with time, and the broad negative band at 1660−1630 cm^{-1}, indicating the loss of the random coil structure (see Figure S2 and Table S1, Supporting Information, for kinetic constants).

Following the same procedure in the preparation of the $Aβ(12\text{-}28)_u$ peptide stock solution, in ∼30% of the experiments, the β-sheet band was found at 1627 cm^{-1} upon first and second flashes and remained at this position throughout the kinetic experiment (Figure S4, Supporting Information). The observation of the 1627 cm^{-1} band in two subsequent flashes for $Aβ(12\text{-}28)_u$ is in contrast to $Aβ(12\text{-}28)_p$. Even after extra ice sonication (1 min) of these peptide stock solutions, we obtained the β-sheet band at 1627 cm^{-1} in both flashes.

Nature of the β Sheets. As mentioned in the Introduction, concurrent occurrences of a strong band near 1630−1620 cm^{-1} and a distinct band around 1690 cm^{-1} indicate the formation of antiparallel β sheets, whereas for the parallel β sheets, a distinct band at 1690 cm^{-1} is missing. The presence of the 1687 cm^{-1} photolysis band makes it difficult to distinguish between the different β sheets in the described experiments. However, as discussed earlier, subtraction of the photolysis signals indicates the formation of antiparallel β sheets when $Aβ(12\text{-}28)_p$ and $Aβ(12\text{-}28)_u$ aggregate.

To independently confirm the antiparallel nature of the β sheet in the aggregates, we used the reducing agent dithiothreitol (DTT), which reacts with the photolysis byproduct 2-nitrosoacetophenon and removes the band at 1687 cm^{-1}. This reaction is associated with an increase in absorption at 1642 cm^{-1}, as shown in Figure 4A for an NPE sulfate experiment without peptide. Also, in the presence of protected peptide, a similar band at 1645 cm^{-1} in the red spectrum (0.69−7.5 s after the flash) of Figure 4B is seen and gives evidence for the DTT reaction with the initial photoproduct 2-nitrosoacetophenone. Bands at 1477 and 1452 cm^{-1} in this spectrum (not shown) indicate formation of the intermediate 2-hydroxylaminoacetophenone[53] at the recording time of this spectrum, while formation of the final product 3-methylanthranil[53] is monitored by a slowly developing 1466 cm^{-1} band in the later spectra (not shown). Although the reduction by DTT removes the 1687 cm^{-1} band of the initial photolysis product 2-nitrosoacetophenone, a weak band remained at 1686 cm^{-1} in the presence of peptide, which can, therefore, be assigned to the aggregated peptides.

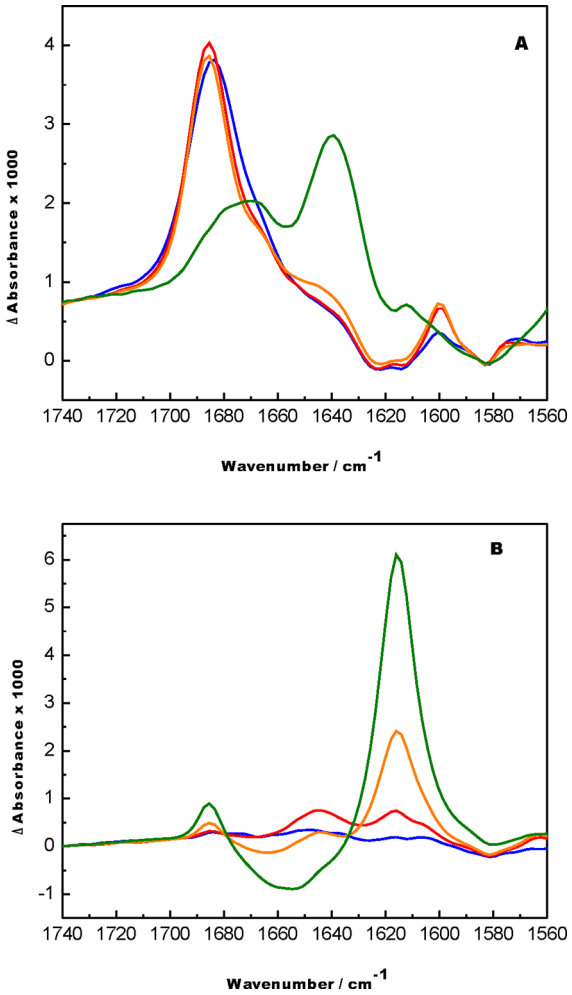

Figure 4. Infrared difference spectra obtained in the presence of 60 mM DTT in D_2O. The color code for the spectra is the same as that in Figure 2A; the orange spectrum was recorded 7.5−76 s after the photolysis flash. (a) First flash on 60 mM NPE sulfate. (b) Second flash on an $Aβ(12\text{-}28)_p$ sample in the presence of NPE sulfate.

Interestingly, the main band at 1616 cm^{-1} rises slower than in the experiments without DTT and hardly shifts with time. This implies extended β-sheet formation on the seconds time scale and that the conditions in our DTT samples have influenced the aggregation process.

The spectra shown in Figure 4B were obtained upon the second flash. No aggregation was observed after the first flash. This might be due to the need of protonating DTT's thiol groups, which have pK_a values of 9−10.

The observations made for the protected peptide in the presence of DTT after the second flash were made for the unprotected fragment upon the first and the second flashes. Thus, an aggregation induced by a sudden pH jump in $Aβ(12\text{-}28)_u$ also causes a transformation of random coil structures to antiparallel β-sheet structures (see Figure S5, Supporting Information).

The appearance of the 1687 cm^{-1} band in the DTT experiments along with the strong band at 1617 cm^{-1} (Figure 4B) is characteristic for the formation of antiparallel β sheets. For this assignment to be safe, the 1687 cm^{-1} band needs to be a distinct band and well separated from other absorption at lower wavenumbers. Although this seems to be the case for the later spectra in Figure 4B, difference spectra can be deceiving,

dx.doi.org/10.1021/jp305015g | J. Phys. Chem. B 2012, 116, 12389−12397

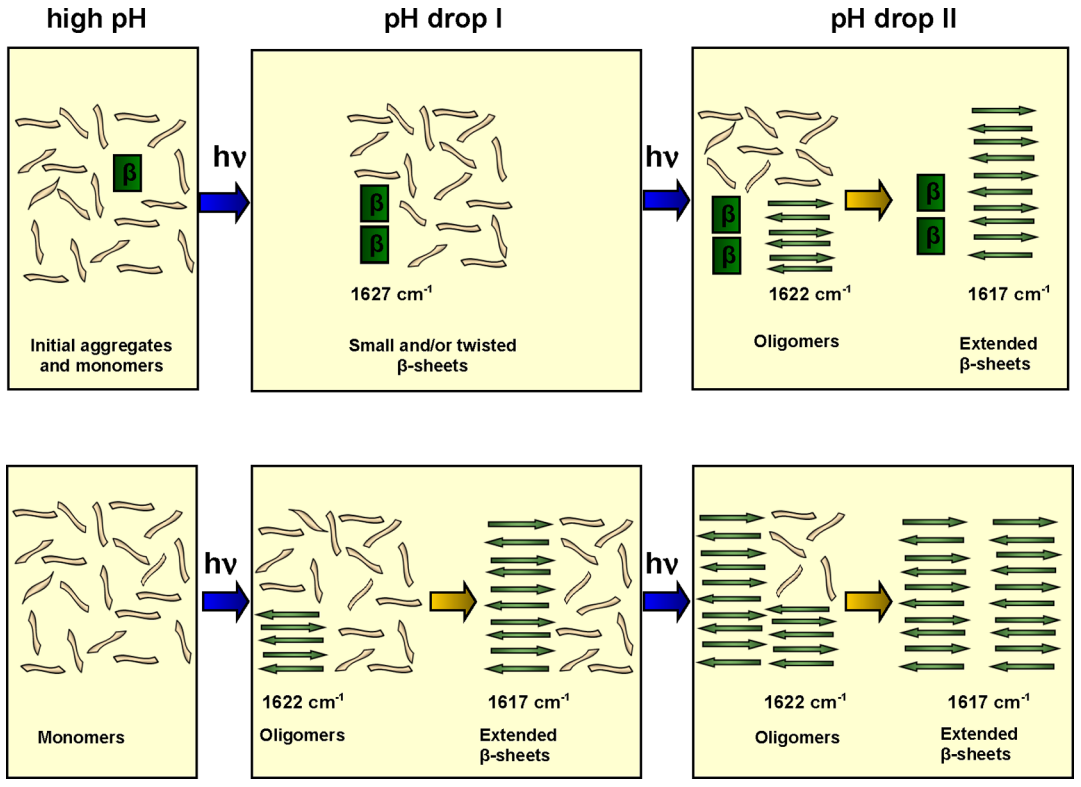

Figure 5. Cartoon representation of the aggregation processes in protected Aβ(12-28) triggered by two pH jumps. Top: samples with initial aggregates giving rise to 1627 cm^{-1} aggregates in flash 1 and to 1617 cm^{-1} aggregates in flash 2. Bottom: extra-sonicated samples without initial aggregates, giving the 1617 cm^{-1} aggregates in both flashes.

and the apparent distinctness of a positive band can rather be caused by adjacent negative bands. Therefore, a distinct positive band of a reaction product in a difference spectrum does not necessarily reflect a property of the product spectrum. Because of this, we seeked further confirmation for an assignment to antiparallel β sheets by fitting the difference spectrum and by constructing absorption spectra of the aggregates as described in the Supporting Information based on our difference spectra and two different published parameter sets for the unstructured peptide.[38,55]

The constructed absorption spectra of the aggregates are shown in Figure S6 (Supporting Information). They show a clear and distinct 1685 cm^{-1} band. Therefore, we can safely conclude that the 1617 cm^{-1} A$\beta(12\text{-}28)_p$ aggregates contain antiparallel β sheets. The intensity ratio between high and low wavenumber components is 4.5, which is somewhat lower than the value of 5.5 inferred from the spectrum of the β-barrel protein OmpF[19] with almost entirely antiparallel β sheets. Thus, the 1617 cm^{-1} oligomers of A$\beta(12\text{-}28)_p$ are predominantly composed of antiparallel β sheets.

DISCUSSION

Overview. Our CD and IR absorption spectra are in line with the known pH dependence of Aβ(12-28), which is predominantly unstructured at basic and strongly acidic pH values but adopts a β-sheet structure at slightly acidic pH values.[46] Time-resolved FTIR spectroscopy in combination with a photoinduced pH jump enabled us to monitor the formation of the early oligomers of Aβ(12-28) aggregation. Figure 5 gives a cartoon representation of the observed aggregation processes, as explained in the following section. Experiments with both protected and unprotected Aβ(12-28) indicated two types of β-sheet-containing oligomers characterized by different amide I absorption maxima at 1627 and 1617 cm^{-1}. This has been observed before for Aβ(11-28),[39] but not in our previous work on Aβ(1-28), where the 1627 cm^{-1} type aggregates were not observed.[40]

Effects of End Protection. For A$\beta(12\text{-}28)_u$ and A$\beta(12\text{-}28)_p$, we found the same two types of aggregates as indicated by the same amide I maxima. However, a striking difference was that the same aggregates were formed in consecutive flashes for A$\beta(12\text{-}28)_u$, whereas different aggregates formed for A$\beta(12\text{-}28)_p$. This shows that charges at the peptide ends do not influence the structure, but the propensity for adopting a given structure. The latter effect could be explained by the presence of electrostatic attractive forces between the differently charged unprotected ends of this peptide when the strands are in an antiparallel orientation. We conclude that the protected and the unprotected Aβ(12-28) are capable of forming the same types of aggregates, indicating that the charges at the ends of the unprotected peptide have little effect on the structure of the oligomers. However, they affect the propensity to adopt a certain structure.

1627 cm^{-1} Aggregates. The 1627 cm^{-1} band forms rapidly at pH ~ 8.2. Its position suggests that the β sheets are more twisted and/or have less strands than the 1617 cm^{-1} aggregates. The 1627 cm^{-1} band does not shift with time, indicating no further addition of strands to the existing β sheets. The 1627 cm^{-1} aggregates do not form at the expense of the random coil structure, which is concluded from the absence of a negative band describing a decrease in the random coil conformation at 1660−1640 cm^{-1}. The fast kinetics of formation, the missing of a random coil band, and the absence of the 1627 cm^{-1} band upon additional sonication all point

dx.doi.org/10.1021/jp305015g | J. Phys. Chem. B 2012, 116, 12389−12397

toward the involvement of pre-existing aggregates. Therefore, the 1627 cm^{-1} band might be caused either by the formation of aggregates from pre-existing aggregates or by a conformational change of these aggregates. That the 1627 cm^{-1} band is observed upon the first flash for Aβ(12-28)$_p$, that is, at a higher pH than the 1617 cm^{-1} aggregates, can be explained by a higher pK_a of the histidines or a lower pK_a of the lysines in the existing aggregates as compared to the unstructured monomers.

Interestingly, the band position observed here for the main band (1627 cm^{-1}) and that for the small band that remained after subtraction of the photolysis contribution (1697 cm^{-1}, the presence of this band could not be established unequivocally because of its small amplitude) match with those found for oligomers of the full-length peptide Aβ(1-42) (1630 and 1695 cm^{-1}).[19] The spectrum of these oligomers resembles most closely that of the β-barrel protein OmpF, and, therefore, it was hypothesized that the Aβ oligomers form β barrels that generate pores in biological membranes and thereby become toxic.[19] The spectral similarities with the 1627 cm^{-1} aggregates make β barrels also a structural possibility for the Aβ(12-28) peptide. The central portion of this peptide—Aβ(16-22)—formed β barrels in Monte Carlo simuations[56] in which individual peptides adopt a linear conformation. The Aβ(12-28) peptide adopts hairpin conformations in molecular dynamics simulations with a bend close to residue 20.[50,51] This makes possible a β-barrel structure similar to a short version of the hemolysin β barrel (pdb entry 7AHL[57]). Here, 7 monomers adopt hairpin structures in the β-barrel domain to form an antiparallel β sheet with 14 strands. The bend is at residues 128−129, and the height of the β-barrel portion formed by the 17 residues, 121−137, is ∼24 Å. This is somewhat less than the thickness of the hydrophobic core of biological membranes, but only 2 Å less than the length of the gramicidin channel.[58] Therefore, a β-barrel structure for Aβ(12-28) that forms pores in membranes seems to be conceivable.

1617 cm^{-1} Aggregates. The 1617 cm^{-1} aggregates form by initial rapid oligomerization, followed by a slower growth to larger aggregates after a pH drop from ∼8.2 to 4−5. The strand orientation in their β sheets is antiparallel, as indicated by the absorption change near 1687 cm^{-1} in the slow phase of the experiment, by subtraction of the photolysis contribution to the spectra and by the experiments with DTT. This is in line with current knowledge that shorter fragments of Aβ generally tend to form antiparallel β sheets.[8−14] The 1617 cm^{-1} aggregates assemble from unstructured monomers and turn to relatively planar and large β sheets according to the low wavenumber of the β-sheet band. In the absence of DTT, its position shifts from initially 1622 to 1617 cm^{-1} with time, indicating association of further peptides with the sheets, since the wavenumber is expected to shift down when the number of strands increases.[32,40,59] The downshift increases the splitting between low and high wavenumber bands. Here, the splitting between low and high wavenumbers was 62 cm^{-1} initially and increased to 69 cm^{-1} within 12 s. This is similar to our previous work on Aβ(1-28), where the splitting was 63 cm^{-1} initially and increased to 67 cm^{-1}, and suggests that the number of strands in β sheets of the early oligomers, formed within 60 ms of the pH jump, is close to 5−10.[40]

CONCLUSIONS

Time-resolved FTIR spectroscopy in combination with a photoinduced pH jump monitored the formation of the early oligomers of Aβ(12-28) aggregation in aqueous solution. The results highlight the complexity of Aβ aggregation, since two types of aggregates were observed that differ in their amide I band position, pH profile, kinetics of formation, size, and ability to grow. The structure of those aggregates is encoded in the sequence of the peptide and not influenced by charges at the ends.

MATERIALS AND METHODS

Reagents. Aβ (12-28)$_p$ and Aβ (12-28)$_u$ were purchased from NeoMPS (Group SNPE, Strasbourg, France), deuterated water was purchased from Cambridge Isotope Laboratories, Inc. (Andover, MA), dithiothreitol from Molecular Sigma Biology (Canada), and 4-methylimidazole from Aldrich (Steinheim, Germany).

Peptide Sample Preparation. The peptide was dissolved by 1 min of ice sonication in 10 mM NaO^2H at a peptide concentration of 1 mM. The pH of this solution was around 9, as determined by pH paper. Samples for CD and infrared (IR) absorption measurements were prepared as follows: phosphate buffer at different pH values (final concentration = 60 mM) was dried on a CaF_2 window with a 30 μm trough, rehydrated with 1 μL of Aβ(12-28) (1 mM) and 1.5 μL of ^2H_2O (final peptide concentration = 400 μM), and closed with a flat CaF_2 window. As an exception, the pH 9 samples were prepared without buffer. Samples for time-resolved IR experiments did not contain buffer, instead 15 μL of 10 mM NPE sulfate (final concentration = 60 mM) was dried and rehydrated with peptide and ^2H_2O, as described above.

FTIR and CD spectra shown in Figure 1 were obtained with freshly prepared samples. For the experiments with the protected peptide that gave the 1627 aggregates in the first flash (Figure 2), two of three experiments were performed within 1 h of peptide preparation. One of the samples was stored at −20 °C and measured after 5 days. The same is true for the experiments that gave the 1617 cm^{-1} aggregates in the first flash (Figure 3). We detected no difference between the freshly prepared and the stored samples. The DTT experiment shown in Figure 4 was done with a sample that was stored for 15 days. For the unprotected peptide, two of three experiments that produced the 1617 cm^{-1} aggregates (Figure S2, Supporting Information) were done with samples stored for 1 day, while the third was stored for nearly a month; and two of three samples that gave the 1627 cm^{-1} aggregates (Figure S3, Supporting Information) were freshly prepared, while the third was stored for 7 days. The DTT experiment with the unprotected peptide (Figure S5, Supporting Information) was performed with a sample that was stored for 6 days.

CD Measurements. A Chirascan CD spectrometer from Applied Photophysics and a TC-125 temperature controller were employed to record CD spectra. The spectral range was 180−300 nm, which required 2 min for each scan. Each spectrum is the average of 10 scans. The temperature was set at 22 °C. The same sample in the same 30 μm demountable CaF_2 cuvette was used for CD and FTIR measurements.

FTIR Measurements. Spectra were recorded with a Bruker IFS66 spectrometer equipped with HgCdTe detector at a 4 cm^{-1} spectral resolution and a zero filling factor of 2. The recording time was 60 ms per interferometer scan, and the Blackman-Harris 3-term apodization function was used. For absorption spectra, the same sample was used as for the CD measurements. For time-resolved experiments, the sample was equilibrated at 22 °C for 15 min in the spectrometer and a reference spectrum (1000 scans) was recorded before applying

dx.doi.org/10.1021/jp305015g | J. Phys. Chem. B 2012, 116, 12389−12397

a flash from a Xenon flash tube filtered by a Schott UG11 filter (~20% photolysis). Time-resolved rapid scan spectra were acquired in the following way: 10 single-scan spectra between 2 and 674 ms (start and end times of spectra recording); 10 spectra of 10 scans each between 0.69 and 7.5 s; 10 spectra of 100 scans each between 7.5 and 76 s; and 20 spectra of 500 scans each between 76 and 760 s. With both protected and unprotected peptides, we repeated the photolysis experiment with three different samples, and the figures presented here represent the average of these three experiments, except for the spectra in Figures 2C and 4B, which show results from single experiments. In the case of Figure 2C, the other two experiments gave similar spectra; however, the ratio of peptide versus photolysis bands was somewhat smaller than that for the spectra shown. In the case of Figure 4B, only a single experiment was performed.

Data Analysis. Integration of the IR difference bands was performed with respect to a baseline drawn between the average absorption in spectral ranges on both sides of the bands with the OPUS software. The parameters used are listed in Table 2. The kinetic traces were fitted by triple exponentials.

Table 2. Parameters for the Integration of Difference Bands[a]

	band position (cm^{-1})		
	1617	1627	1643
integration range	1612−1625	1614−1635	1639−1653
baseline point 1	1630	1770	1770
baseline point 2	1625	1750	1750
baseline point 3	1609	1638	1577
baseline point 4	1600	1631	1552

[a]The baseline points were calculated from the points listed in the table as follows. The absorbance value of baseline point A was calculated from the listed points 1 and 2 by averaging the absorbance in the range between points 1 and 2. The wavenumber of A was set to that of point 2. For baseline point B, the range between points 3 and 4 was averaged and the wavenumber of point 3 used. A baseline was then drawn between points A and B.

■ ASSOCIATED CONTENT

Supporting Information

The Supporting Information describes the method to eliminate the photolysis bands in the amide I region, the results with the unprotected peptide, and the construction of peptide absorption spectra from the difference spectra. This material is available free of charge via the Internet at http://pubs.acs.org.

■ AUTHOR INFORMATION

Corresponding Author

*E-mail: barth@dbb.su.se.

Notes

The authors declare no competing financial interest.

■ ACKNOWLEDGMENTS

We thank Anna Wahlström and Astrid Gräslund for valuable discussions. This work was financed by a research grant from Alzheimerfonden and the spectrometer by Knut och Alice Wallenbergs Stiftelse.

■ REFERENCES

(1) Selkoe, D. J. *Phys. Rev.* **2001**, *81*, 741−766.
(2) Laczkó, I.; Vass, E.; Soós, K.; Fülöp, L.; Zarándi, M.; Penke, B. *J. Pept. Sci.* **2008**, *14*, 731−741.
(3) Krysmann, M. J.; Castelletto, V.; Hamley, I. W. *Soft Matter* **2007**, *3*, 1401−1406.
(4) Jarvet, J.; Damberg, P.; Bodell, K.; Göran Eriksson, L. E.; Gräslund, A. *J. Am. Chem. Soc.* **2000**, *122*, 4261−4268.
(5) Eanes, E. D.; Glenner, G. G. *J. Histochem. Cytochem.* **1968**, *16*, 673−677.
(6) Harper, J. D.; Lansbury, P. T., Jr. *Annu. Rev. Biochem.* **1997**, *66*, 385−407.
(7) Goedert, M.; Spillantini, M. G. *Science* **2006**, *314*, 777−781.
(8) Petty, S. A.; Decatur, S. M. *J. Am. Chem. Soc.* **2005**, *127*, 13488−13489.
(9) Petkova, A. T.; Ishii, Y.; Balbach, J. J.; Antzutkin, O. N.; Leepman, R. D.; Delaglio, F.; Tyko, R. *Proc. Natl. Acad. Sci. U.S.A.* **2002**, *99*, 16742−16747.
(10) Lührs, T.; Ritter, C.; Adrian, M.; Riek-Loher, D.; Bohrmann, B.; Döbeli, H.; Schubert, D.; Riek, R. *Proc. Natl. Acad. Sci. U.S.A.* **2005**, *102*, 17342−17347.
(11) Lansbury, P. T.; Costa, P. R.; Griffiths, J. M.; Simon, E. J.; Auger, M.; Halverson, K. J. *Nat. Struct. Biol.* **1995**, *2*, 990−998.
(12) Halverson, K.; Fraser, P. E.; Kirschner, D. A.; Lansbury, P. T. *Biochemistry* **1990**, *29*, 2639−2644.
(13) Rabanal, F.; Tusell, J. M.; Sastre, L.; Quintero, M. R.; Cruz, M.; Grillo, D.; Pons, M.; Albericio, F.; Serratosa, J.; Giralt, E. *J. Pept. Sci.* **2002**, *8*, 578−588.
(14) Tycko, R.; Ishii, Y. *J. Am. Chem. Soc.* **2003**, *125*, 6606−6607.
(15) Hardy, J.; Selkoe, D. J. *Science* **2002**, *297*, 353−356.
(16) Kirkitadze, M. D.; Bitan, G.; Teplow, D. B. *J. Neurosci. Res.* **2002**, *69*, 567−577.
(17) Lazo, N. D.; Maji, S. K.; Fradinger, E. A.; Bitan, G.; Teplow, D. B. The Amyloid *β* Protein. In *Amyloid Proteins: The ß Sheet Conformation and Disease*; Sipe, J. D., Ed.; Wiley-VCH Verlag Gmbh & Co: Weinheim, Germany, 2005; pp 385−491.
(18) Haass, C.; Selkoe, D. J. *Nat. Rev. Mol. Cell Biol.* **2007**, *8*, 101−112.
(19) Cerf, E.; Sarroukh, R.; Tamamizu-Kato, S.; Breydo, L.; Derclaye, S.; Dufrêne, Y. F.; Narayanaswami, V.; Goormaghtigh, E.; Ruysschaert, J. M.; Raussens, V. *Biochem. J.* **2009**, *421*, 415−423.
(20) Hoyer, W.; Grönwell, C.; Jonsson, A.; Ståhl, S.; Härd, T. *Proc. Natl. Acad. Sci. U.S.A.* **2008**, *105*, 5099−5104.
(21) Walsh, D. M.; Hartley, D. M.; Kusumoto, Y.; Fezoui, Y.; Condron, M. M.; Lomakin, A.; Benedek, G. B.; Selkoe, D. J.; Teplow, D. B. *J. Biol. Chem.* **1999**, *274*, 25945−25952.
(22) Soto, C.; Castaño, E. M.; Frangione, B.; Inestrosa, N. C. *J. Biol. Chem.* **1995**, *270*, 3063−3067.
(23) Huang, T. H. J.; Yang, D. S.; Plaskos, N. P.; Go, S.; Yip, C. M.; Fraser, P. E.; Chakrabatty, A. *J. Mol. Biol.* **2000**, *297*, 73−87.
(24) Benseny-Cases, N.; Cócera, M.; Cladera, J. *Biochem. Biophys. Res. Commun.* **2007**, *361*, 916−921.
(25) Barth, A. *Biochim. Biophys. Acta* **2007**, *1767*, 1073−1101.
(26) Khurana, R; Fink, A. L. *Biophys. J.* **2000**, *78*, 994−1000.
(27) Susi, H.; Byler, D. M. *Arch. Biochem. Biophys.* **1987**, *258*, 465−469.
(28) Chitnumsub, P.; Fiori, W. R.; Lashuel, H. A.; Diaz, H.; Kelly, J. W. *Bioorg. Med. Chem.* **1999**, *7*, 39−59.
(29) Hahn, S.; Kim, S.-S.; Lee, C.; Cho, M. *J. Chem. Phys.* **2005**, *123*, 084905.
(30) Strasfeld, D. B.; Ling, Y. L.; Gupta, R.; Raleigh, D. P.; Zanni, M. T. *J. Phys. Chem. B* **2009**, *113*, 15679−15691.
(31) Kubelka, J.; Keiderling, T. A. *J. Am. Chem. Soc.* **2001**, *123*, 12048−12058.
(32) Chirgadze, Y. N.; Nevskaya, N. A. *Biopolymers* **1976**, *15*, 627−636.
(33) Yamada, N.; Ariga, K.; Naito, M.; Matsubara, K.; Koyama, E. *J. Am. Chem. Soc.* **1998**, *120*, 1212−12199.
(34) Toniolo, C.; Palumbo, M. *Biopolymers* **1977**, *16*, 219−224.
(35) Decatur, S. M. *Acc. Chem. Res.* **2006**, *39*, 169−175.

(36) Hiramatsu, H.; Kitagawa, T. *Biochim. Biophys. Acta* **2005**, *1753*, 100−107.
(37) Zandomeneghi, G.; Krebs, M. R. H.; McCammon, M. G.; Fändrich, M. *Protein Sci.* **2004**, *13*, 3314−3321.
(38) Eker, F.; Griebenow, K.; Schweitzer-Stenner, R. *Biochemistry* **2004**, *43*, 6893−6898.
(39) Juszczyk, P.; Kołodziejczyk, A. S.; Grzonka, Z. *J. Pept. Sci.* **2009**, *15*, 23−29.
(40) Perálvarez-Marín, A.; Barth, A.; Gräslund, A. *J. Mol. Biol.* **2008**, *379*, 589−596.
(41) Barth, A.; Corrie, J. E. T. *Biophys. J.* **2002**, *83*, 2864−2871.
(42) Barth, A.; Kreutz, W.; Mäntele, W. *FEBS Lett.* **1990**, *277*, 147−150.
(43) Cepus, V.; Ulbrich, C.; Allin, C.; Troullier, A.; Gerwert, K. *Methods Enzymol.* **1998**, *291*, 223−245.
(44) Barth, A. In *Dynamic Studies in Biology: Phototriggers, Photoswitches and Caged Biomolecules. Time-Resolved Infrared Spectroscopy with Caged Compounds*; Goeldner, M., Givens, R., Eds.; Wiley-VCH: Weinheim, Germany, 2005; pp 369−399.
(45) Barth, A.; Zscherp, C. *FEBS Lett.* **2000**, *477*, 151−156.
(46) Fraser, P. E.; Nguyen, J. T.; Surewicz, W. K.; Kirschner, D. A. *Biophys. J.* **1991**, *60*, 1190−1201.
(47) Esler, W. P.; Stimson, E. R.; Ghilardi, J. R.; Vinters, H. V.; Lee, J. P.; Mantyh, P. W.; Maggio, J. E. *Biochemistry* **1996**, *35*, 749−757.
(48) Gorevic, P. D.; Castano, E. M.; Sarma, R.; Frangione, B. *Biochem. Biophys. Res. Commun.* **1987**, *147*, 854−862.
(49) Rabanal, F.; Tusell, J. M.; Sastre, L.; Quintero, M. R.; Cruz, M.; Grillo, D.; Pons, M.; Albericio, F.; Serratosa, J.; Giralt, E. *J. Pept. Sci.* **2002**, *8*, 578−588.
(50) Simona, F.; Tiana, G.; Brogila, R. A.; Colombo, G. *J. Mol. Graphics Modell.* **2004**, *23*, 263−273.
(51) Baumketner, A.; Shea, J.-E. *J. Mol. Biol.* **2006**, *362*, 567−579.
(52) Tamm, L. K.; Tatulian, S. A. *Q. Rev. Biophys.* **1997**, *30*, 365−429.
(53) Barth, A.; Corrie, J. E. T.; Gradwell, M. J.; Maeda, Y.; Mäntele, W.; Meier, T.; Trentham, D. R. *J. Am. Chem. Soc.* **1997**, *119*, 4149−4159.
(54) Barth, A.; Mantele, W.; Kreutz, W. *Biochim. Biophys. Acta* **1991**, *1057*, 115−123.
(55) Chirgadze, Y. N.; Shestopalov, B. V.; Venyaminov, S. Y. *Biopolymers* **1973**, *12*, 1337−1351.
(56) Irbäck, A.; Mitternacht, S. *Proteins* **2008**, *71*, 207−214.
(57) Song, L.; Hobaugh, M. R.; Shustak, C.; Cheley, S.; Bayley, H.; Gouaux, J. E. *Science* **1996**, *274*, 1859−66.
(58) Kelkar, D. A.; Chattopadhyay, A. *Biochim. Biophys. Acta* **2007**, *1768*, 2011−2025.
(59) Lee, C.; Cho, M. *J. Phys. Chem. B* **2004**, *108*, 20397−20407.